J. Phycol. **52,** 888–895 (2016)

DOI: 10.1111/jpy.12435

NOTE

ASTERIONELLOPSIS TROPICALIS (BACILLARIOPHYCEAE): A NEW TROPICAL SPECIES FOUND IN DIATOM ACCUMULATIONS[1]

Andréa de Oliveira da Rocha Franco[2]

Institute of Oceanography, Federal University of Rio Grande - FURG, Av. Itália, km8, CEP 96203-900, Rio Grande, Brazil

Ng Haig They

Department of Oceanography and Limnology, Federal University of Rio Grande do Norte-UFRN, Av. Senador Dinarte de Medeiros Mariz, s/n, Praia de Mãe Luiza, CEP 59014-002, Natal/RN, Brazil

Luis Gustavo de Castro Canani

Institute of Water Sciences and Technology, Federal University of Oeste do Pará - UFOPA, Av. Mendonça Furtado, 2946, CEP 68040-050, Santarém, Brazil

Rodrigo Maggioni

Institute of Marine Sciences, Federal University of Ceará - UFC, Av. da Abolição, 3207, CEP 60165-081, Fortaleza, Brazil

and Clarisse Odebrecht

Institute of Oceanography, Federal University of Rio Grande - FURG, Av. Itália, km8, CEP 96203-900, Rio Grande, Brazil

The diatom *Asterionellopsis glacialis* sensu lato forms high-density patches in the surf zone of some sandy beaches worldwide and was until recently considered a cosmopolitan species. With the recent description of four cryptic species, the identity of specimens found in these accumulations remains uncertain. In this study, diatom patches were sampled from two sandy beaches of the Brazilian coast: one tropical (Futuro Beach, 3° S; 38° W) and one subtropical (Cassino Beach, 32° S; 52° W). Fine structure of frustules and the sequencing of three phylogenetic markers revealed the subtropical strains to be *A. guyunusae* and the tropical strains to be a new species, here described as *Asterionellopsis tropicalis* sp. nov. *A. tropicalis* was differentiated morphologically by the number of striae in 10 µm at the foot pole and head (39–44; 38–45, respectively), from *A. lenisilicea* (46–55; 46–64), *A.* maritima (46–51; 46–60), and *A. thurstonii* (42–58; 55–70). The number of striae at the head region of the valvocopula (10 µm) helped to distinguish *A. tropicalis* (56–62) from *A. guyunusae* (61–64), but *A. tropicalis* was morphologically undistinguishable from *A. glacialis*. The sequence divergence from other identified *Asterionellopsis* species was 13%–16% (*Cox1*), 11%–12% (5.8S + ITS2) and 2%–6% (*RbcL*), and *A. tropicalis* formed a distinct monophyletic clade with high support in all analyzed phylogenetic trees (single or multi-locus). This work will aid in the understanding of the ecological and physiological diversity of diatom patches that are key to the trophic webs of sandy beaches.

Key index words: **araphid diatom; Cryptic species; diatom patches; phylogeny; surf zone**

***Abbreviations*: 5.8S + ITS2, region that codes the 5.8S rRNA and internal transcribed spacer region 2; B, maximum width of the foot pole; BOLD, The Barcode of Life Data Systems; bp, base pairs; CB, Cassino Beach; C, culture frustules; *Cox1*, gene for subunit 1 of the enzyme cytochrome c oxidase, from the mitochondrial genome; dNTPs, deoxyribonucleotide triphosphate; E, environment frustules; FB, Futuro Beach; Ho, height of the framework foot ocellus; H, orthogonal height foot pole; Max, maximum; Min, minimum; M, mean; NE-Brazil, Northeast Brazil; N, number of measurements; PEG, polyethylene glycol; *RbcL*, gene for the large subunit of the enzyme ribulose 1,5-bisphosphate carboxylase oxygenase, from the chloroplast genome; Wo, width of the framework foot ocellus**

The diatom *Asterionellopsis glacialis* (Castracane) Round was considered to be cosmopolitan, sometimes abundant in plankton in cold and temperate coastal waters (Hasle and Syvertsen 1996) and accumulating in the surf zone on sandy beaches in all ocean basins including tropical regions on the east coast of South America (Odebrecht et al. 2014).

[1]Received 30 July 2015. Accepted 12 May 2016.
[2]Author for correspondence: e-mail andrea_lisandra@hotmail.com.
Editorial Responsibility: R. Wetherbee (Associate Editor)

TABLE 1. Strains of *Asterionellopsis* used in the genetic analysis, date of isolation, geographical location and number of sequence access in GenBank or BOLD.

Species/Strain Date of isolation	Collection site Lat. and Log.	*Cox1*	ITS1 + 5.8S + ITS 2	*RbcL*
[a]*A. tropicalis* ASTTRO1 03/2014	Futuro Beach, Brazil 3°41′ S; 38°27′ W	KT351586	KT336328	–
[a]*A. tropicalis* ASTTRO2 03/2014	Futuro Beach, Brazil 3°41′ S; 38°27′ W	[b]KT351587	[b]KT336329	[b]KT336325
[a]*A. guyunusae* ASTGUY1 09/2012	Cassino Beach, Brazil 32°12′ S; 52°10′ W	KT285183	–	–
[a]*A. guyunusae* ASTGUY2 06/2014	Cassino Beach, Brazil 32°12′ S; 52°10′ W	[b]KT336323	[b]KT336326	[b]KT336324
[a]*A. guyunusae* ASTGUY3 06/2014	Cassino Beach, Brazil 32°12′ S; 52°10′ W	KT343751	KT336327	–
A. guyunusae UR1 2009	Montevideo, Uruguay 34°57′ S; 56°9′ W	–	KF454002	–
A. guyunusae UR8 2009	Montevideo, Uruguay 34°57′ S; 56°9′ W	[b]KF453984	[b]KF454003	[b]KF453990
A. thurstonii CCMP135 na	Black Sea ~43°00′ N; ~34°00′ E	[b]KF453985	[b]GQ330311	[b]KF453991
A. thurstonii CCMP1581 01/1992	Renesee, Netherlands 51°43′ N; 3°46′ E	KF453986	GQ330312	KF453992
A. lenisilicea MB9 2009	Maces Bay, Canada 45°5′ N; 66°28′ W	KF453981	–	–
A. lenisilicea MB8 2009	Maces Bay, Canada 45°5′ N; 66°28′ W	[b]KF453980	–	–
A. lenisilicea MB7 2009	Maces Bay, Canada 45°5′ N; 66°28′ W	–	[b]KF453999	[b]KF453987
A. maritima HX5 2009	Bedford, Canada 44°24′ N; 63°40′ W	[b]KF453982	[b]KF454000	[b]KF453988
A. maritima EC114(4) 009	Saint Jonh's, Canada 47°33′ N; 52°42′ W	KF453983	KF454001	KF453989
A. glacialis KMCCB296 1999	Samcheonpo, Japan 34°55′ N; 128°4′ E	–	–	[b]HQ710592
A. cf. *glacialis* CCMP139	Bay California, Mexico 24°16′ N; 111°31′ W	[c,b]ASTBR022-13	[b]FJ864272	KF453993
Dimeregramma acutum Van5.3 05/2010	Vancouver, Canada 49°1′ N; 123°6′ W	[b]KF768027	[b]KF454004	[b]KF453994

[a]Strains and sequences obtained from this study.
[b]Sequences used in concatenated tree.
[c]Number of access from public database of the BOLD system (The Barcode of Life Data Systems).

Diatom accumulations in the surf zone of sandy beaches are visible as brown/orange/greenish colored patches formed by the high density of diatoms, up to 10^9 cells $\cdot$ L^{-1} (Campbell 1996), and are important for primary production, contributing to the diet of metazoans (Abreu et al. 2003, Netto and Meneghel 2014). In a recent study, Kaczmarska et al. (2014) described four new cryptic species from *A. glacialis* sensu lato strains, isolated from the Black Sea, the Pacific and Atlantic oceans, primarily from temperate regions. However, which *A. glacialis* sensu lato species are able to form accumulations in the surf zone remain unknown.

Studies on the biogeography and phylogeny of marine diatoms are deficient in information from low latitude environments (20° S–20° N). For example, studies on gene flow in *Pseudo-nitzschia* Peragallo (Casteleyn et al. 2010), morphological diversification and genetic divergence of *Asterionellopsis* (Kaczmarska et al. 2014), biogeography of *Skeletonema* Greville (Kooistra et al. 2008) and Pleistocene distribution of diatoms on a large scale (Cermeño and Falkowski 2009) all lack information for the tropical regions. However, tropical and subtropical regions may support high phytoplankton diversity (Clayton et al. 2013), and the acquisition of information on these populations is critical to the understanding of global diversity, biogeography, and speciation processes in the oceans.

The objective of this study was to identify the species of *Asterionellopsis* that were present in surf diatom accumulations on tropical and subtropical sandy beaches of the east coast of South America using morphological (fine structure) and molecular tools (nucleus, mitochondrion, and chloroplast genes).

Five strains of *Asterionellopsis* were isolated from diatom accumulations in the surf zone of two sandy beaches in Brazil: two strains from the tropical Futuro Beach (3° S, 38° W) and three strains from the subtropical Cassino Beach (32° S, 53° W; Table 1). Using a micropipette, single colonies were isolated, and cultures maintained in f/2 medium prepared with offshore water (Guillard 1975) plus sodium silicate (1.06×10^{-4} M; final concentration)

(Andersen 2005) and salinity of 28–35. Irradiance (190 μmol photons $\cdot m^{-2} \cdot s^{-1}$; 12:12 dark:light) and temperature (20°C–23°C) were controlled in incubators at the Marine Microalgae Culture Collection at Federal University of Rio Grande.

DNA from the *Asterionellopsis* pellets obtained from centrifugation (2576 *g*; 5 min) of cultures of each strain was extracted with the commercial DNeasy® Plant Mini Kit (Qiagen, Hilden, Germany) and stored at −20°C. The DNA fragments were amplified from three regions: (i) the internal transcribed spacer region, including the ITS1 + 5.8S + ITS2, (ii) the region of the chloroplast genome that codes for the large subunit of enzyme ribulose 1,5-bisphosphate carboxylase oxygenase (*RbcL*), and (iii) the region of the mitochondrial genome that codes for the enzyme cytochrome c oxidase subunit 1 (*Cox1*). The PCR amplification of the ITS1 + 5.8S + ITS2 and *RbcL* fragments were conducted in 25 μL volumes containing one unit of Platinum Taq DNA Polymerase (Invitrogen Carlsbad, California, USA), 1.5 mM $MgCl_2$, 0.2 μM of each primer, 0.2 mM dNTPs, and 1.0 μL of extracted DNA. The *Cox1* PCR was performed in 25 μL that contained one unit of Platinum Taq DNA Polymerase (Invitrogen, Carlsbad, California, USA), 1.5 mM $MgCl_2$, 0.6 mM of each primer, 0.2 mM dNTPs, and 1–2 μL of extracted DNA. The primers used are listed in Table S1 in the Supporting Information.

All fragments were amplified in a thermocycler (The Veriti Dx ™ 96-Well Thermal Cycler) with an initial denaturation at 94°C for 2 min. The amplification of ITS1 + 5.8S + ITS2 and *RbcL* PCR strictly followed the procedures used by Lang and Kaczmarska (2011). For the *Cox1* fragments, the initial denaturation was followed by 30 cycles of denaturation (94°C, 30 s), annealing (48°C, 30 s), and extension (72°C, 1 min), with a final 10 min extension at 72°C (modified from Iwatani et al. 2005). The purification of DNA fragments by selective precipitation with the addition of PEG followed the recommendations of Hartley and Bowen (1996). The PCR products were sequenced using a BigDye Terminator v3.1 Cycle Sequencing Kit (Life Technologies, Carlsbad, California, USA), following the manufacturer's instructions. The sequenced products were purified by centrifugation in isopropanol and were read in an ABI 3500 automated capillary sequencer (Applied Biosystems, Foster City, CA, USA).

The sequences were manually edited and aligned using the algorithm Clustal W with the software MEGA 6 (Thompson et al. 1997). Divergence between the sequences was calculated with a simple distance for pairs of sequences (Tamura et al. 2013); the uncorrected distance (p-distance) method was chosen because the method was more appropriate for comparisons of closely correlated species (Nei and Kumar 2000). The divergence was calculated for the fragments: 5.8S + ITS2, *Cox1*, and *RbcL*, because just these fragments have p-distance values available in the literature for comparison. Four phylogenetic trees were constructed, one for each gene individually and the other with three concatenated genes. The analyses involved 12, 14, and 11 sequences of the fragments of ITS1 + 5.8S + ITS2, *Cox1*, and *RbcL*, respectively, obtained in this study, in addition to other available sequences in GenBank. *Dimeregramma acutum* Hustedt was included as outgroup for all phylogenetic trees of *Asterionellopsis* (Kooistra et al. 2009, Ashworth et al. 2012, Table 1). The nucleotide substitution model that was the best fit for each data matrix was estimated using the Akaike Information Criterion (Akaike 1974) by the software JModeltest 2.1 (Table S2 in the Supporting Information). The concatenated tree was constructed with a best fit model for each part of matrix (gene; Table S2).

The Bayesian analysis (Markov Chain Monte Carlo method) with two independent runs, four chains of one million generations each, one topology sampled each 100 generations and a discard of 25%, was performed using the software MrBayes 3.2.3. (Ronquist and Huelsenbeck 2003) The convergence between independent runs, the discard of generations and the analysis performance were validated with the likelihood plots for each run and the effective sample size (>200) using the software Tracer 1.5 (Rambaut and Drummond 2007).

Morphometric analyses were carried out on *Asterionellopsis* frustules present in natural samples fixed with 4% buffered formaldehyde from the surf zone of Futuro Beach (May 6, 2012) and Cassino Beach (1990; August 27, 2004; April 15, 2012). The Cassino Beach samples were part of the Brazilian Long-Term Ecological Research collection. Cells in culture were measured after 6 months for the tropical strains, and three (ASTGUY2, ASTGUY3) and 21 (ASTGUY1) months for subtropical strains. The pellets (field and strain samples) were subjected to oxidation with hydrogen peroxide and hydrochloric acid and were then washed with distilled water to remove the organic matter from the frustules (Simonsen 1974). A drop of clean diatom concentrate was pipetted onto a cover slip attached to the electron microscope stub with a carbon adhesive and after drying (50°C) the stubs were coated with gold (Denton Vaccum Desk V sputter coater) and examined under the SEM (JEOL JSM – 6610 LV, JEOL, Akshima, Japan) operating at 25–30 kV and 9 mm working distance.

The SEM images of at least 30 frustules of the field samples and of 15 frustules of each *Asterionellopsis* strain were measured using AxioVision Zeiss, Oberkochen, Germany software. When possible, the apical cell length, head width, number of striae in 10 μm along the foot pole sternum, number of striae and spines in 10 μm of the head, number of striae in 10 μm along of the foot region of the valvocopula, number of striae in 10 μm along the head region of the valvocopula, number of slits in the foot pole ocellus, width and height of the framework surrounding the foot ocellus, the

maximum width of the foot pole and the orthogonal foot pole height were determined. The last two measurements were proposed by Kaczmarska et al. (2014) (Fig. S1 in the Supporting Information). The ratios between the maximum foot pole width and the orthogonal height and between the width and the height of the surrounding of the ocellus were also calculated. Nomenclature followed Round et al. (1990) and Kaczmarska et al. (2014).

Three and two sequences of *Cox1* were obtained from strains isolated from the subtropical Cassino Beach and the tropical Futuro Beach respectively. Two sequences of the ITS1 + 5.8S + ITS2 fragment were obtained from each beach, and one sequence corresponding to a part of the *RbcL* gene was also obtained from each beach (Table 1). Phylogenetic trees and values of the p-distance were obtained by comparing our sequences with available sequences in the Genbank and BOLD; the alignment size was: 418 bp for *Cox1*, 458 bp for 5.8S + ITS2 (with gaps), 449 bp for *RbcL* and 823 pb for ITS1 + 5.8S + ITS2 (with gaps).

Apical length, number of spines on the head (10 μm), number of slits in foot ocellus, the width (Wo), height (Ho) of the foot ocellus, Wo:Ho ratio, the width (B) and height (H) of the foot pole and B: H ratio from field samples showed different values than strains of *A. tropicalis* and *A. guyunusae*, obtained from Futuro Beach and Cassino Beach respectively (Table 3). Some of these differences might have been caused by allometric changes due to cell size reduction in culture. However, the number of striae in 10 μm at the foot pole, the head and corresponding valvocopula was similar between field and strain samples (Table 3), indicating that these measures are more stable and useful in the anatomic characterization of *Asterionellopsis* species. However, the overlap in minima and maxima values of most morphological characters of the tropical and subtropical strains hampers their use for species differentiation (Table 3). The number of striae in 10 um at the head valvocopula was the character with the smallest overlap between the tropical strains/field samples (56–62/61–62) and *A. guyunusae* (61–64/62–64; Table 3).

Comparison of sequences of the three strains isolated from Cassino Beach with the other *Asterionellopsis* species available in GenBank resulted in a monophyletic group with *A. guyunusae* Luddington. The posterior probabilities of 1.0, 1.0, 0.97 and 1.0 in the trees, respectively, of *Cox1*, ITS 1 + 5.8S + ITS2, *RbcL* and the three concatenated fragments, and the genetic divergence of 0% for the three studied genes, confirmed the identification of these strains as *A. guyunusae*.

The two strains from the tropical Futuro Beach were highly divergent compared to species known to date; the divergence ranged from 13% to 16% for the *Cox1*, 11%–12% for the 5.8S + ITS2 and 2%–6% for the *RbcL* (Table 2). Tropical strains formed a distinct monophyletic clade with high support (posterior probability = 1) in all analyzed phylogenetic trees (single or multi-locus), confirming that their identity is unknown (Figs. 1 and S2 in the Supporting Information).

TABLE 2. Divergence (%) obtained from the pairwise uncorrected distance among the sequences of *Asterionellopsis* species.

	Cox1	5.8S + ITS 2	RbcL
A. tropicalis versus *A. glacialis*	0.15	0.11	0.02
A. tropicalis versus *A. guyunusae*	0.15	0.11	0.04
A. tropicalis versus *A. lenisilicea*	0.16	0.14	0.06
A. tropicalis versus *A. maritima*	0.16	0.13	0.05
A. tropicalis versus *A. thurstonii*	0.13	0.12	0.02
A. guyunusae versus *A. lenisilicea*	0.10–0.11	0.10	0.03
A. guyunusae versus *A. maritima*	0.11	0.08	0.04
A. guyunusae versus *A. thurstonii*	0.13	0.08	0.03
A. guyunusae versus *A. glacialis*	0.12	0.05	0.02
A. glacialis versus *A. lenisilicea*	0.10–0.11	0.07	0.04
A. glacialis versus *A. maritima*	0.10	0.06	0.03
A. glacialis versus *A. thurstonii*	0.14	0.08	0.03
A. maritima versus *A. lenisilicea*	0.09	0.02	0.03
A. maritima versus *A. thurstonii*	0.13	0.10	0.04
A. thurstonii versus *A. lenisilicea*	0.12–0.13	0.12	0.05

Based on the data above we propose that the tropical strains are of an unknown cryptic species, which we here describe as new species.

Asterionellopsis tropicalis Franco, **sp. nov.** Diagnosis: Morphological signature: *A. tropicalis* (Fig. 2) has fewer striae in 10 μm at the foot pole (39–44) and head (38–45) than other species described by Kaczmarska et al. (2014), *A. lenisilicea* (foot pole 46–55; head 46–64), *A. maritima* (foot pole 46–51; head 46–60) and *A. thurstonii* (foot pole 46–51; head 55–70). In spite of a small overlap, the number of striae in 10 μm at the head region of the valvocopula aids in the separation of *A. tropicalis* (56–62) from *A. guyunusae* (61–64). However, we did not find a morphological character that would differentiate *A. tropicalis* from *A. glacialis*.

Holotype: Deposited at the collection of the Herbarium Prof. Dr. Alarich Schultz (Zoobotanic Foundation, Rio Grande do Sul, Brazil) ASTTRO2: HAS 6.717.

Isotype and Paratype: Deposited at the collections of the Herbarium Prof. Dr. Alarich Schultz (Zoobotanic Foundation, Rio Grande do Sul, Brazil) ASTTRO2 (Isotype): HAS 6.718, HAS 6.719; ASTTRO1 (Paratype): HAS 6.720, HAS 6.721, HAS 6.722, and the Berlin-Dahlem Botanic Garden and Botanical Museum (BGBM Herbarium) ASTTRO1 (Paratype): B 40 0041507; ASTTRO2 (Isotype): B 40 0041508.

Type locality: Surf zone from Futuro Beach, Fortaleza, Ceará, Brazil (3°41′ S, 38°27′ W). Etymology: Reference to the climate of the geographical location.

Description: Valves heteropolar, basal pole (foot pole) trapezoidal in pleural or girdle view and oval shape in valve view. Thin region (head), two to four times the length of the foot pole, with rimoportula at the apex. Sternum narrow, uniseriate striae

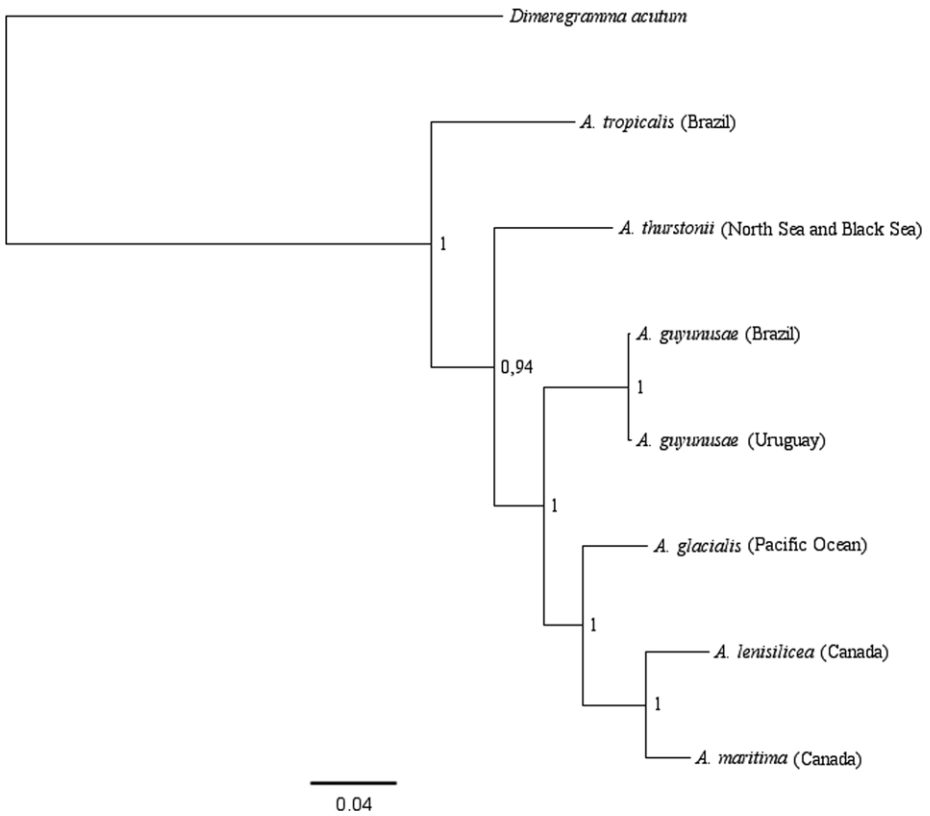

FIG. 1. Bayesian phylogenetic tree of *Asterionellopsis* with three concatenated genes (*Cox1*, ITS1 + 5.8S + ITS2, and *RbcL*).

formed of poroids. Cells united at the foot poles, forming star-shaped (two-dimensional) or spiral (three-dimensional) colonies. Slits form an ocellus at each pole. The ocellus at the foot pole is surrounded by a thick silica framework. Head width 0.4–1.6 μm; 39–44 striae in 10 μm along the foot sternum; 38–45 striae in 10 μm along the head; 56–64 striae in 10 μm at the foot region of the valvocopula; 56–62 striae in 10 μm at the head region of the valvocopula; 5–7 spines in 10 μm at the head; 9–13 slits on foot ocellus (Table 4; Fig. 2).

Distribution: To date, identified at the surf zone of the tropical Futuro Beach.

Asterionellopsis tropicalis was found in high cell densities in the surf zone of the tropical Futuro Beach, Brazil, indicating that its environmental requirements differ from those of the other known *Asterionellopsis* species (subtropical and temperate type locality) (Kaczmarska et al. 2014). *A. tropicalis* was distinguished from the other species of the genus by the large genetic distance found for the markers *RbcL* (0.02–0.06), *Cox1* (0.13–0.16), and 5.8S + ITS2 (0.11–0.14) within the typical range of diatom species differentiation (Evans et al. 2007, Moniz and Kaczmarska 2009, MacGillivary and Kaczmarska 2011). In addition, the 5.8S + ITS2 divergence between other *Asterionellopsis* species was low (>0.11; Table 2), but presented differences in the secondary structure of the helices II and III of the ITS2 (Kaczmarska et al. (2014), which are typically correlated with reproductive isolation in diatoms (Amato et al. 2007). We used all 5.8S + ITS2 fragments and compared genetic distance (diatom barcoding) according to Moniz and Kaczmarska (2009). Different values of the 5.8S + ITS2 divergence than these obtained in the present study resulted from manually improving alignments with the aid of conserved regions found in the ITS2 secondary structure by Kaczmarska et al. (2014).

The trees constructed for individual genes showed a monophyletic group for both Brazilian tropical strains with high support (posterior probability = 1) for the ITS1 + 5.8S + ITS2 and the *Cox1*. For the *RbcL*, although obtained from one strain only, a distinct branch was also formed (Fig. S2). The tree with the three concatenated fragments (*Cox1*, *RbcL*, and ITS1 + 5.8S + ITS2; alignment 1,690 bp with gaps) also showed a monophyletic branch for *A. tropicalis* (Fig. 1).

The metric values of morphological features were different between field samples (Futuro Beach and Cassino Beach) and strains obtained from each beach and differences among *A. guyunusae* strains from Uruguay (Kaczmarska et al. 2014) and Brazil (present study) in size of the apical length, head width, height and width of the foot pole and their ratio (B:H), indicating that these allometric measures are of low taxonomic value. The foot ocellus

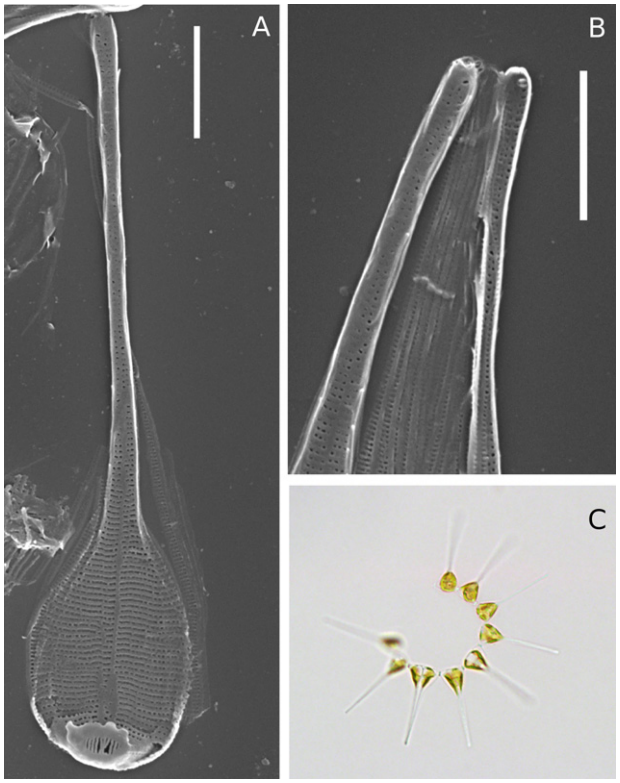

FIG. 2. *Asterionellopsis tropicalis* (ASTTRO2 strain) (A) external view; (B) external view (left), valvocopula with band (mid) and internal view (right) from the head, (C) *A. tropicalis* cells in chain; 5 μm bar.

size/shape also showed high morphological variation, even among individuals of the same strain (Tables 3 and 4). However, the number of striae on the valve and valvocopula of foot pole and head varied less among *A. guyunusae* strains from Uruguay and Brazil; these characteristics were similar between field samples and strains obtained from each beach (Tables 3 and 4). Thus, striae on the valve and valvocopula are useful morphological characters in *Asterionellopsis* species.

The best morphological characteristic that differentiated *A. tropicalis* from other species of the genus was the number of striae in 10 μm at the foot pole and/or head: *A. tropicalis* (foot 39–44; head 38–45), *A. lenisilicea* (foot 46–55; head 46–64), *A. maritima* (foot 46–51; head 46–60), *A. thurstonii* (foot 46–51; head 55–70). Despite the small overlap in striae density at the head region of the valvocopula between *A. tropicalis* (56–62) and *A. guyunusae* (61–64), these taxa could be discriminated morphologically (Table 4). Similarly, the morphological distinction of some pseudo-cryptic species of *Pseudo-nitzschia* required the analysis of the valvocopula fine structure (Lundholm et al. 2002, 2006). We suggest that the valvocopula of other *Asterionellopsis* species are examined in the future. In the process of speciation, genetic divergence precedes morphological differentiation, thus explaining why

TABLE 3. Minimum (Min), maximum (Max), and the number of measurements (N) made of each morphological characteristic from *Asterionellopsis tropicalis* and *A. guyunusae* in culture samples and *Asterionellopsis* from the environment, Futuro Beach (FB) or Cassino Beach (CB).

	A. tropicalis Strain Min–Max (*N*) [FB Min–Max (*N*)]	*A. guyunusae* Strain Min–Max (*N*) [CB Min–Max (*N*)]
Apical length	24.6–41.2 (30) [a][39.5–70.1 (26)]	14.4–38.8 (49) [a][24.8–95.3(38)]
Striae beside sternum foot pole (10 μm)	39–44 (30) [40–44 (28)]	41–47 (50) [42–46 (36)]
Striae at the head (10 μm)	38–45 (28) [40–45 (27)]	40–48 (35) [41–44 (11)]
Striae along the foot region of the valvocopula (10 μm)	56–64 (17) [59–62 (12)]	58–64 (16) [62–64 (6)]
Striae along the head region of the valvocopula (10 μm)	56–62 (11) [61–62 (7)]	61–64 (8) [62–64 (15)]
Spines at the head (10 μm)	5–7 (5) [a][6–9 (14)]	5–9 (9) [a][3–6 (28)]
Maximum width of the foot pole (B)	7.0–7. 9 (3) [a][8.2–8.7 (3)]	7.3–10.1 (9) [9.2]
Orthogonal height foot pole (H)	4.0–4.2 (3) [a][4.5–5.5 (3)]	3.6–5.2 (9) [5.7]
B:H – Foot pole	1.7–1.9 (3) [a][1.5–1.8 (3)]	1.7–2.4 (9) [a][1.6]
Number of slits on foot ocellus	9–13 (12) [9–13 (14)]	7–12 (24) [a][8–15 (20)]
Height of the framework foot ocellus (Ho)	1.3–2.0 (6) [a][2.1–2.4 (3)]	1.2–1.8 (16) [a][2.2–3.7 (12)]
Width of the framework foot ocellus (Wo)	2.6–3.7 (6) [2.9–3.2 (3)]	1.8–3.0 (15) [a][2.6–4.4 (13)]
Wo/Ho – Ocelli	1.5–2.2 (6) [a][1.3–1.5 (3)]	1.1–1.7 (15) 1.2 [a][0.7–1.4] (12)
Head width	0.4–1.6 (28) [0.5–0.7 (29)]	0.3–1.2 (45) [0.3–0.8 (30)]

[a]Measurements from field samples, Fututo Beach or Cassino Beach, were different than strains obtained from each beach, *A. tropicalis* or *A. guyunusae* respectively.

phylogenetically closely related species are indistinguishable by morphology (Leliaert et al. 2014). *A. tropicalis* and *A. glacialis* are morphologically indistinct, however, the phylogenetic analysis indicated that they were not sister species, as was observed for *Pseudo-nitzschia arenysensis* Quijano-Scheggia, Garcés, Lundholm, and *Pseudo-nitzschia delicatissima* (Cleve) Heiden (Quijano-Scheggia et al. 2009). An extreme example can be found in *Nitzschia inconspicua* (morpho-species), which is paraphyletic, i.e., some clones form a monophyletic group with other *Nitzschia* and *Denticula* species (Rovira et al. 2015).

Asterionellopsis glacialis sensu lato is an important component of the marine phytoplankton (Leblanc et al. 2012) and also forms visible patches of brown/orange color in the surf zone of several sandy beaches around the world (Campbell 1996, Odebrecht et al. 2014). Recently, four new cryptic

TABLE 4. Comparison of the number of striae in 10 μm, ratio between the foot width (B) and height (H), and the number of spines on the head of *Asterionellopsis* species.

	Striae (10 μm)					
	Sternum foot	Sternum head	Foot region of the valvocopula	Head region of the valvocopula	B:H foot	Spines on the head (10 μm)
A. guyunusae (Brazil)	41–47	40–48	58–64	61–64	1.7–2.4	5–9
[b]*A. guyunusae* (Uruguay)	41–50	44–60	[a]– [a]–	[a]– [a]–	~1.5	4–9
A. tropicalis	39–44	38–45	56–64	56–62	1.7–1.9	5–7
[b]*A. lenisilicea*	46–55	46–64	[a]–	[a]–	1.6–1.9	6–16
[b]*A. maritima*	46–51	46–60	[a]–	[a]–	1.6–1.8	5–12
[b]*A. thurstonii*	46–51	46–60	[a]–	[a]–	1.6–1.8	5–12
[b]*A. glacialis*	36–50	42–70	[a]–	[a]–	~1.0–1.1	3–10

[a]No information.
[b]Data from Kaczarmska et al. 2014.

species were identified in this group (Kaczmarska et al. 2014) and we observed another one summing up now six *Asterionellopsis* species. At present, which *Asterionellopsis* species enable to form diatom accumulations in the surf zone of sandy beaches are unknown. The reliable identification of surf diatoms is essential for species biogeography and because of their ecological importance in the trophic webs of sandy beaches (Abreu et al. 2003, Netto and Meneghel 2014). In addition, little is known about the physiology of surf diatoms and studies require species identification.

On the Brazilian coast, the strains that were isolated from the diatom patches were *A. tropicalis* (new species, described in the present study) and *A. guyunusae*, responsible for diatom accumulations in tropical and subtropical regions respectively. These beaches are ~3,444 km apart from each other and differ largely in environmental features such as water temperature and salinity, which present higher values and smaller amplitude at Futuro Beach (26.7°C–29.9°C; S 34–38; Franco 2013) than Cassino Beach (6°C–29°C; S 14–38; Odebrecht et al. 2010). In addition, diatom accumulations at the latter are more frequent in winter (10°C–15°C; S <25; Odebrecht et al. 2010), confirming that diatom accumulations in the surf zone of both beaches are promoted by different species. *A. glacialis* sensu lato form colored patches in several beaches along the Brazilian coast between Futuro Beach and Cassino Beach (Odebrecht et al. 2014). At present the limits of their spatial distribution and whether *A. tropicalis* and *A. guyunusae* occur together are unknown. The cryptic species coexistence would be explained by biological differences that prevent competitive exclusion (Sáez and Lozano 2005).

Asterionellopsis glacialis sensu lato also forms accumulations in beaches from Oceania, Asia and Africa (Campbell 1996, Odebrecht et al. 2014); molecular information and ultrastructure details of the frustules revealed by SEM from these geographical areas is required for the global understanding of the taxonomy and distribution of the genus. Other surf diatoms are also known to be widely distributed, for example, *Anaulus australis* Drebes and Schulz and *Aulacodiscus kittonii* Arnott ex Ralfs were recorded on the coasts of South America, South Africa and Oceania, and *Attheya armata* (West) Crawford was found on the coasts of North America (Pacific), Europe, the Canary Islands and Argentina in the Atlantic Ocean (Odebrecht et al. 2014). It is possible that these surf diatoms include cryptic or pseudo-cryptic species, considering the large geographical distances and the wide range of environmental conditions. We suggest that surf diatoms present a high diversification potential, and therefore, their species identification and determination of the phylogeny would help to understand the patterns of speciation and biogeography observed for marine microorganisms in general.

The authors thank the Plankton Laboratory team of the Institute of Marine Sciences of the Federal University of Ceará for sampling and samples shipment. We are grateful to P.C. Abreu for the support provided, the Brazilian National Council of Science and Technology (CNPq) for fellowships to A.O.R.F. and C.O., and the Brazilian Long-term Ecological Research (PELD CNPQ Proc. 403805/2012-0). To the anonymous reviewers, our gratitude for their time donated and relevant suggestions.

Abreu, P. C., Rörig, L. R., Garcia, V., Odebrecht, C. & Biddanda, B. 2003. Decoupling between bacteria and the surf-zone diatom *Asterionellopsis glacialis* at Cassino Beach, Brazil. *Aquat. Microb. Ecol.* 32:219–28.

Akaike, H. 1974. A new look at the statistical model identification. *IEEE Trans. Autom. Control* 19:716–23.

Amato, A., Kooistra, W. H. C. F., Ghiron, J. H. L., Mann, D. G., Pröschold, T. & Montresor, M. 2007. Reproductive isolation among sympatric cryptic species in marine diatoms. *Protist* 158:193–207.

Andersen, R. A. 2005. *Algal Culturing Techniques*. Elsevier Academic Press, Amsterdam, 596 pp.

Ashworth, M. P., Ruck, E., Lobban, C. S., Romanovicz, D. K. & Theriot, E. C. 2012. A revision of the genus *Cyclophora* and description of *Astrosyne* gen. nov. (Bacillariophyta), two genera with the pyrenoids contained within pseudosepta. *Phycologia* 51:684–99.

Campbell, E. E. 1996. The global distribution of surf diatom accumulations. *Rev. Chil. Hist. Nat.* 69:495–501.

Casteleyn, G., Leliaert, F., Backeljau, T., Debeer, A. E., Kotaki, Y., Rhodes, L., Lundholm, N., Sabbe, K. & Vyvermanet, W. 2010. Limits to gene flow in a cosmopolitan marine planktonic diatom. *Proc. Natl. Acad. Sci. USA* 107:12952–7.

Cermeño, P. & Falkowski, P. G. 2009. Controls on diatom biogeography in the ocean. *Science* 325:1539–41.

Clayton, S., Dutkiewicz, S., Jahn, O. & Follows, M. J. 2013. Dispersal, eddies, and the diversity of marine phytoplankton. *Limnol. Oceanogr. Fluids Environ.* 3:182–97.

Evans, M. K., Wortley, A. H. & Mann, G. D. 2007. An assessment of potential diatom "barcode" genes (cox1, rbcL, 18S and ITS rDNA) and their effectiveness in determining relationships in *Sellaphora* (Bacillariophyta). *Protist* 158:349–64.

Franco, A. O. R. 2013. *Variação temporal e espacial das acumulações de diatomáceas (manchas marrons) em uma praia tropical de mesomaré, Praia do Futuro (Fortaleza Ceará).* Monography in Oceanography. Federal University of Ceará, Fortaleza, Brazil, 87 pp.

Guillard, R. R. L. 1975. Culture of phytoplankton for feeding marine invertebrates. *In* Smith, W. L. & Chanley, M. H. [Eds.] *Culture of Marine Invertebrate Animals.* Springer, New York, pp. 29–60.

Hartley, J. L. & Bowen, H. 1996. PEG precipitation for selective removal of small DNA fragments. *Focus* 18:27.

Hasle, G. R. & Syvertsen, E. E. 1996. Marine diatoms. *In* Tomas, C. R. [Ed.] *Identifying Marine Diatoms and Dinoflagellates.* Academic Press, San Diego, California, pp. 5–385.

Iwatani, N., Murakami, S. & Suzuki, Y. 2005. A sequencing protocol of some DNA regions in nuclear, chloroplastic and mitochondrial genomes with an individual colony of *Thalassiosira nordenskioeldii* Cleve (Bacillariophyceae). *Polar Biosc.* 18:35–45.

Kaczmarska, I., Mather, L., Luddington, I. A., Muise, F. & Ehrman, J. M. 2014. Cryptic diversity in a cosmopolitan diatom known as *Asterionellopsis glacialis* (Fragilariaceae): implications for ecology, biogeography, and taxonomy. *Am. J. Bot.* 101:267–86.

Kooistra, W. H. C. F., Forlani, G. & De Stefano, M. 2009. Adaptation of araphid pennate diatoms to a planktonic existence. *Mar. Ecol.* 30:1–15.

Kooistra, W. H. C. F., Sarno, D., Balzano, S., Gu, H., Andersen, R. A. & Zingone, A. 2008. Global diversity and biogeography of *Skeletonema* species (Bacillariophyta). *Protist* 159:177–93.

Lang, I. & Kaczmarska, I. 2011. A protocol for a single-cell PCR of diatoms from fixed samples: method validation using *Ditylum brightwellii* (T. West) Grunow. *Diatom Res.* 26:43–9.

Leblanc, K., Arístegui, J., Armand, L., Assmy, P., Beker, B., Bode, A., Breton, E. et al. 2012. A global diatom database – abundance, biovolume and biomass in the world ocean. *Earth Syst. Sci. Data Discuss.* 5:147–85.

Leliaert, F., Verbruggen, H., Vanormelingen, P., Steen, F., López-Bautista, J. M., Zuccarello, G. C. & Clerck, O. 2014. DNA-based species delimitation in algae. *Eur. J. Phycol.* 49:179–96.

Lundholm, N., Hasle, G. R., Fryxell, G. A. & Hargraves, P. E. 2002. Morphology, phylogeny and taxonomy of species within the *Pseudo-nitzschia americana* complex (Bacillariophyceae) with descriptions of two new species, *Pseudo-nitzschia brasiliana* and *Pseudo-nitzschia linea*. *Phycologia* 41:480–97.

Lundholm, N., Moestrup, Ø., Kotaki, Y., Hoef-Emden, K., Scholin, C. & Miller, P. 2006. Inter- and intraspecific variation of the *Pseudo-nitzschia delicatissima* complex (Bacillariophyceae) illustrated by rRNA probes, morphological data and phylogenetic analyses. *J. Phycol.* 42:464–81.

MacGillivary, M. L. & Kaczmarska, I. 2011. Survey of the efficacy of a short fragment of the rbcL gene as a supplemental DNA barcode for diatoms. *J. Eukaryot. Microbiol.* 58:529–36.

Moniz, M. B. J. & Kaczmarska, I. 2009. Barcoding diatoms: is there a good marker? *Mol. Ecol. Resour.* 9:65–74.

Nei, M. & Kumar, S. 2000. *Molecular Evolution and Phylogenetics.* Oxford University Press, New York, 328 pp.

Netto, S. A. & Meneghel, A. 2014. Pulse of marine subsidies: the role of surf diatom *Asterionellopsis glacialis* accumulations in structuring the meiofauna of sandy beaches. *Mar. Biodiv.* 44:445–57.

Odebrecht, C., Bergesch, M., Rörig, L. R. & Abreu, P. C. 2010. Phytoplankton interannual variability at Cassino Beach, Southern Brazil (1992-2007), with emphasis on the surf zone diatom *Asterionellopsis glacialis*. *Estuar. Coast.* 33:570–83.

Odebrecht, C., Du Preez, D. R., Abreu, P. C. & Campbell, E. E. 2014. Surf zone diatoms: a review of the drivers, patterns and role in sandy beaches food chains. *Estuar. Coast. Shelf Sci.* 150:24–35.

Quijano-Scheggia, S. I., Garcés, E., Lundholm, N., Moestrup, Ø., Andree, K. & Camp, J. 2009. Morphology, physiology, molecular phylogeny and sexual compatibility of the cryptic *Pseudo-nitzschia delicatissima* complex (Bacillariophyta), including the description of *P. arenysensis* sp. nov. *Phycologia* 48:492–509.

Rambaut, A. & Drummond, A. J. 2007. *Tracer, version 1.5.* Available at:http://tree.bio.ed.ac.uk/software/tracer/ (last accessed 1 December 2014)

Ronquist, F. & Huelsenbeck, J. P. 2003. MrBayes 3: Bayesian phylogenetic inference under mixed models. *Bioinformatics* 19:1572–4.

Round, F. E., Crawford, R. M. & Mann, D. G. 1990. *The Diatoms Biology and Morphology of the Genera.* Cambridge University Press, Cambridge, 747 pp.

Rovira, L., Trobajo, R., Sato, S., Ibàñez, C. & Mann, D. G. 2015. Genetic and physiological diversity in the diatom *Nitzschia inconspicua*. *J. Eukaryot. Microbiol.* 62:815–32.

Sáez, A. G. & Lozano, E. 2005. Cryptic species: as we discover more examples of species that are morphologically indistinguishable, we need to ask why and how they exist. *Nature* 433:111.

Simonsen, R. 1974. *The Diatom Plankton of the Indian Ocean Expedition of RV "Meteor" 1964-1965 (Meteor Forschungsergebnisse).* Gebrüder Borntraeger, Berlin, 107 pp.

Tamura, K., Stecher, G., Peterson, D., Filipski, A. & Kumar, S. 2013. MEGA6: molecular evolutionary genetics analysis version 6.0. *Mol. Biol. Evol.* 30:2725–9.

Thompson, J. D., Gibson, T. J., Plewniak, F., Jeanmougin, F. & Higgins, D. G. 1997. The CLUSTAL X windows interface: flexible strategies for multiple sequence alignment aided by quality analysis tools. *Nucleic Acids Res.* 25:4876–82.

Supporting Information

Additional Supporting Information may be found in the online version of this article at the publisher's web site:

Figure S1. Measures of *Asterionellopsis* frustules: (A) valve view (1) apical length; (2) head width; (3) maximum foot width; (4) foot orthogonal height; (B) (5) width of the ocellus framework; (6) height of the ocellus framework; (C) girdle view (7) striae at the head valvocopula.

Figure S2. Bayesian phylogenetic trees of *Asterionellopsis* with posterior probability values, each gene separately constructed with: (A) *Cox1* (418 bp), (B) ITS1 + 5.8S + ITS2 (823 bp), and (C) *RbcL* (449 bp).

Table S1. Primers used for the amplification of ITS1 + 5.8S + ITS2, *Cox1,* and *RbcL.*

Table S2. Selected models for each gene alignment of *Asterionellopsis* sequences with the outgroup (*Dimeregramma acutum*), following the models of Posada (2003).